CALIBRATION OF CO-LOCATED CORRELATION RADIOMETERS FOR THE CASE OF IGNORABLE CROSSTALK

H. Brian Sequeira¹, Corina Nafornita², Peter Vouras³

¹Johns Hopkins University Applied Physics Laboratories, Baltimore, MD 20723, USA
²Communications Dept., Politehnica University of Timisoara, Romania
³Department of Defense, USA

ABSTRACT

We propose a calibration method of correlation radiometers for the case when cross-coupling between channels can be ignored. The method requires sources that are stable with respect to temperature, impedance match, and Excess Noise Ratio (ENR). This treatment establishes a rationale for source stability and describes how these desirable characteristics may be realized. Next, it describes a method by which correlation radiometers may be calibrated and compensated for gain and phase imbalance between channels while ignoring the presence of cross-coupling between them.

Index Terms— calibration, correlation, cross-coupling, gain balance, gain compensation, phase balance, radiometer

1. INTRODUCTION

Passive microwave remote sensing using radiometers was used in applications such as early detection of fire [1], forest surveillance [2], imminent volcanic eruptions [3], monitoring distribution and dynamics of ice [4], monitoring of agricultural output [5]. In contrast to this, synthetic aperture radiometry achieves high spatial resolution using interferometric techniques. Although interferometry is a mature technique in radio astronomy, its application to microwave radiometry is relatively recent [6]. The literature available is sparse and confined to narrow enough bands [7][8][9]. The trend towards wider bandwidths [10] to improve temperature and spatial resolution requires correlation among pairs of radiometers that receive the same noise from the scene. Correlation radiometers are needed in this context, as they provide the complex visibility data required for synthetic image reconstruction.

One of the challenges in synthetic aperture radiometry is calibration. Its purpose is to establish the connection between the measured complex correlations with the scene brightness temperature, accounting for gain, phase, and coupling errors [11]. Early works such as Faris [12] laid the theoretical groundwork for correlation radiometer sensitivity and thermal noise considerations, while Dicke [13] introduced key principles of thermal noise mitigation in total

power radiometers that influenced later radiometric system design. In [14], calibration of the two-channel correlation radiometer is done by 180 phase switching with 50% duty cycle of the local oscillator signal in one of the channels, incorporated in the RF (microwave). In [15], a calibration procedure is proposed requiring the injection of three polarized markers. In [16], centralized Pseudo-Random Noise (PRN) signals are used to calibrate correlation radiometers. Another calibration method [17] for polarization correlation millimeter wave radiometers in vacuum chamber consists of one polarization grid, one temperature adjusted targets, and one cold target and doesn't need any unpolarized target when calibrating a polarization correlation radiometer by regulating the physical of calibration targets.

In this paper, we focus on calibration of co-located correlation radiometers, for the case when cross-coupling between channels can be ignored, a configuration increasingly relevant in wideband synthetic aperture systems. The case when crosstalk between channels cannot be ignored is treated in [18].

2. PROPOSED CALIBRATION METHOD FOR IGNORABLE CROSSTALK

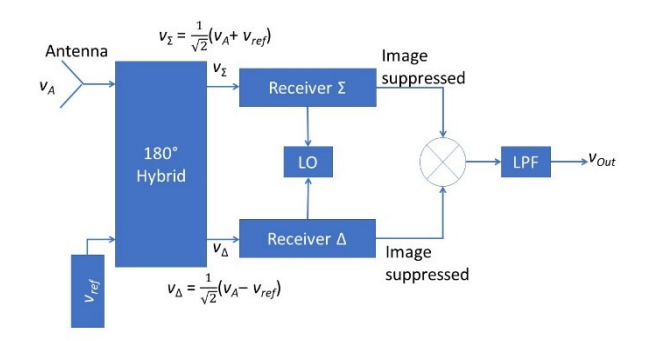


Fig. 1. Simplest form of a correlation radiometer.

Figure 1 shows the simplest form of a correlation radiometer [19]. It consists of two image-reject receivers, Σ and Δ , that are connected to the sum and difference ports of a 180° hybrid coupler. One input of the hybrid is connected to the

antenna whose voltage, v_A , is split equally and in phase at each receiver input. The other input of the hybrid is connected to a reference (calibration) source whose voltage, v_{ref} , is split equally but 180° out of relative phase at the receiver input ports. The receivers are driven by a common local oscillator (LO) to realize image suppressed conversion at intermediate frequency (IF). The image suppressed IF outputs of each receiver are multiplied, and low-pass filtered to produce the correlated output, v_{Out} .

We perform the analysis with voltages, v_A and v_{ref} . We also represent the receivers by amplitude gains, $A_{\Sigma} + \Delta A_{\Sigma}$ and $A_{\Delta} + \Delta A_{\Delta}$, where ΔA_{Σ} and ΔA_{Δ} are complex amplitude gain fluctuations about constant values A_{Σ} and A_{Δ} . All amplitude gains have magnitude and phase and are related to power gain by $G = AA^*$, with A^* being the conjugate of A. With these definitions, the output voltage from the Σ channel is:

$$v_{o\Sigma} = \left(A_{\Sigma} + \Delta A_{\Sigma}\right) \left[\frac{1}{\sqrt{2}} \left(v_{A} + v_{ref}\right) + v_{n\Sigma}\right]$$
 (1)

In (1), $v_{n\Sigma}$ represents the voltage generated by all the receiver's internal noise processes. Likewise, the output voltage from the Δ channel is:

$$v_{o\Delta} = \left(A_{\Delta} + \Delta A_{\Delta}\right) \left[\frac{1}{\sqrt{2}} \left(v_{A} - v_{ref}\right) + v_{n\Delta} \right]$$
 (2)

In (2), $v_{n\Delta}$ represents the voltage generated by all the receiver's internal noise processes. The cross correlation, C_X , between the channels is given by:

$$4RC_{X} = v_{o\Sigma}v_{o\Delta}^{*} = (A_{\Sigma} + \Delta A_{\Sigma})(A_{\Delta}^{*} + \Delta A_{\Delta}^{*})$$

$$\left[\frac{1}{\sqrt{2}}(v_{A} + v_{ref}) + v_{n\Sigma}\right]\left[\frac{1}{\sqrt{2}}(v_{A}^{*} - v_{ref}^{*}) + v_{n\Delta}^{*}\right]$$
(3)

In (3), R is the equivalent Johnson resistor of the radiometer. Evidently, gain fluctuations ΔA_{Σ} and ΔA_{Δ} are uncorrelated with respect to each other as well as to the internal noise $v_{n\Sigma}$ and $v_{n\Delta}$ and these are in turn uncorrelated with voltages from the antenna and reference source v_A and v_{ref} , respectively. So, all of these uncorrelated products vanish and the only term that survives is:

$$4RC_{X} = v_{o\Sigma}v_{o\Delta}^{*} = \frac{1}{2}A_{\Sigma}A_{\Delta}^{*}(|v_{A}|^{2} - |v_{ref}|^{2})$$
 (4)

Several notable observations derive from (4) about the cross-correlation, C_X :

- All internally generated receiver noise regardless of statistical pedigree or spectral character is eliminated in the cross correlator.
- The correlator performs a squaring operation which offers the opportunity for eliminating multiplicative phase noise.
- 3. Correlation further eliminates the effect of gain fluctuations because these are uncorrelated.

4. The phase difference between channels must be small (ideally zero) to obtain good correlation. Clearly, 90° phase difference would cause the correlation to vanish.

Johnson's formula relates the square of a noise voltage to the temperature of the source, e.g., $|v_A|^2 = 4\kappa T_A BR$, and $|v_{Ref}|^2 = 4\kappa T_{Ref}BR$, where κ is Boltzmann's constant, and B is the receiver bandwidth. With this relationship, we write (4) in terms of temperature:

$$C_X = v_{o\Sigma} v_{o\Delta}^* / (4R) = \kappa B A_{\Sigma} A_{\Delta}^* (T_A - T_{ref})$$
 (5)

Observe that this expression supposes that both channels have the same bandwidth. Faris [12] addresses the question of different bandwidths with the interpretation that B is the overlapped portion of each receiver bandwidth. We now describe a method to determine the antenna temperature T_A by toggling T_{ref} between temperatures T_H and T_C . Then from (5),

$$C_H = \kappa B A_{\Sigma} A_{\Delta}^* \left(T_A - T_H \right) \tag{6}$$

$$C_C = \kappa B A_{\Sigma} A_{\Delta}^* (T_A - T_C) \tag{7}$$

We use temperature $T_o = 290$ K, from which excess noise ratio, $ENR = (T_H - T_C)/T_o$, and use this result in the subtraction of (6) from (7) to obtain:

$$C_C - C_H = \kappa T_a B A_{\Sigma} A_{\Lambda}^* (T_H - T_C) / T_a = \kappa T_a B A_{\Sigma} A_{\Lambda}^* ENR$$
 (8)

and

$$A_{\Sigma}A_{\Delta}^{*} = (C_{C} - C_{H})/(\kappa T_{o}B \cdot ENR)$$
 (9)

The denominator on the right-hand side of (9) is real, and so the phase difference between channels is:

$$\Delta \varphi = \arg(A_{\Sigma} A_{\Delta}^*) = \arg(C_C - C_H)$$
 (10)

The cross-correlation gain is,

$$\left| A_{\Sigma} A_{\Delta}^{*} \right| = \sqrt{G_{\Sigma} G_{\Delta}} = G \tag{11}$$

Note that the toggled temperature of the reference (calibration) source permits calculation of the gains of each channel individually, i.e., from the measured difference in noise power under hot and cold states

$$P_{H\Sigma} - P_{C\Sigma} = \kappa B T_o G_{\Sigma} (T_H - T_C) / T_o = \kappa B T_o G_{\Sigma} ENR \quad (12)$$

from which we obtain:

$$G_{\Sigma} = (P_{H\Sigma} - P_{C\Sigma}) / (\kappa B T_o E N R)$$
 (13)

with a similar expression for G_{Δ} . Equation (13) in conjunction with (10) and (11) supplies a basis for

equalizing the gains and compensating for the phase difference between channels. The Σ -channel gain, G_{Σ} , is multiplied by the factor, $\sqrt{G_{\Delta}/G_{\Sigma}}$ $\mathrm{e}^{-J/2\Delta\phi}$. The Δ -channel gain, G_{Δ} , is multiplied by the factor, $\sqrt{G_{\Sigma}/G_{\Delta}}$ $\mathrm{e}^{J/2\Delta\phi}$. With the gain factors so equalized, we define a correlation temperature $T_{corr} = C/(\kappa BG)$, so that from (6), (7) and (11):

$$T_{corr,C} = T_A - T_C \tag{14}$$

$$T_{corr,H} = T_A - T_H \tag{15}$$

Setting $Y = T_{corr,H} / T_{corr,C}$, (14) and (15) yield:

$$T_A = T_C + T_o \frac{ENR}{1 - Y} \tag{16}$$

This expresses T_A in terms of known temperature, T_C , known ENR, and measured Y-factor. It is significant to note that the Y-factor based on correlation temperature can be positive, negative, or even zero, depending on the magnitude of T_A relative to T_H and T_C as evident from (14) and (15). This is unlike the Y-factor of a single receiver for which Y > 1. The reader should recognize the need for proper choice of T_C and ENR of the calibration source described in the next section. The sensitivity of the measurement may be obtained from:

$$\delta T_{corr} = \delta T_A - \delta T_{ref} \tag{17}$$

We add the uncertainties as a root sum of squares because of the independence of the two sources. Thus,

$$\left(\Delta T_{corr}\right)^2 = \left(\Delta T_A\right)^2 + \left(\Delta T_{ref}\right)^2 \tag{18}$$

If $T_{ref} = T_A$, then the sensitivity of this version of a correlation radiometer is $\Delta T_{corr} = \sqrt{2} \Delta T_A$, which is intermediate between ΔT_A for an ideal radiometer and $2\Delta T_A$ for a Dicke radiometer [13].

If the residual gain ratio, $G_{\Sigma}/G_{\Delta} \neq 1$, the sensitivity is impaired from its ideal [20]:

$$\Delta T_{corr} = \sqrt{2}\Delta T_A \sqrt{1 + \left(\sqrt{\frac{G_{\Sigma}}{G_{\Delta}}} - 1\right)^2}$$
 (19)

Throughout this development, we assumed that the characteristics of the reference source, viz., temperature, T_C , and ENR, are perfectly known and the source is perfectly matched to the radiometers over its operating bandwidth, B. None of these assumptions are true in practice, so we turn our attention to how these factors may be mitigated. An example in the next section serves to illustrate how the operation of the radiometer affects requirements posed on the source.

3. INSTRUMENTATION CONSIDERATIONS

This section introduces an analysis of a specific measurement situation that lends insight into the characteristics of instrumentation that is needed to calibrate the radiometer, which are the characteristics of the source: temperature control, ENR stability, and mismatch constancy are matters of interest to the measurement. In a typical scenario, a radiometer points its antenna at a scene of interest that is at some temperature T_{scene} . In the intervening space between the scene and the antenna is a layer through which the noise emitted from the scene propagates. This layer is at some average temperature, T_{atm} , and has some propagation loss, L_{atm} . Consequently, the effective temperature of emission at the antenna input is:

$$T_{emis} = T_{scene} / L_{atm} + T_{atm} \left(1 - 1 / L_{atm} \right)$$
 (20)

The antenna has a collection efficiency, η , and is at a physical temperature, T_A , and the noise temperature immediately after it is,

$$T_{ant} = \eta T_{emis} + (1 - \eta) T_A \tag{21}$$

The noise then propagates through calibration components that have temperature, T_C , and have loss, L_{cal} . Thus, the noise at the receiver input has temperature:

$$T_{in} = T_{ant} / L_{cal} + T_C \left(1 - 1 / L_{cal} \right)$$
 (22)

Temperature T_{in} adds to the excess noise temperature, T_{Rx} , to give the system temperature of the radiometer, i.e.,

$$T_{\text{sys}} = T_{in} + T_{Rx} \tag{23}$$

Clearly, T_{scene} is diluted by a factor $\eta/(L_{atm} L_{cal})$ even as it competes with contributions T_{atm} , T_A , and T_C . The radiometer must be sensitive to changes in T_{scene} amid larger fluctuations from these other sources. It must further endeavor to keep the insertion loss of the calibration circuit low and its temperature as constant as possible relative to the expected range of T_{scene} .

TABLE I. Temperature excursions of scene, atmosphere, antenna, and system temperature

Condition	$T_{scene}\left(\mathbf{K}\right)$	$T_{atm}\left(\mathbf{K}\right)$	$T_A(K)$	$T_{sys}(K)$
Sunlight	300	250	400	1034.25
Shadow	270	240	200	985.60

TABLE II. Change in system temperature for 1K excursions of T_{SCORS} , T_{Allm} , T_A , and T_C in Table I

OI I scene, I a	1 1 scene, 1 atm, 1 A, and 1 C in 1 abic 1				
Condition	∂T_{scene}	∂T_{atm}	∂T_A	∂T_C	
Sunlight	0.26	0.585	0.175	1.5	
Shadow	0.26	0.585	0.175	1.5	

A quantitative understanding of these factors may be gained from the output (Tables I & II) of a simulation that examines a specific example of a radiometer operating under the following conditions: $L_{atm} = 1.25$ (1 dB), $\eta = 0.65$, $L_{cal} = 2$ (3 dB), $T_C = 300$ K, receiver noise figure, $F_{Rx} = 2$ (3 dB) and other temperature excursions in sunlight and shadow. These simulations are based on (20) through (23).

A particularly large excursion of temperature occurs with an antenna on a spacecraft platform that orbits around Earth. Such antenna experiences temperatures as high as 400 K when exposed to sunlight and 200 K when the spacecraft is in Earth's shadow. Table II lists deviations in system temperature for 1 K change off nominal for each of T_{scene} , T_{atm} , T_A , and T_C , with the other temperatures set at nominal. Table II reveals at once that 1 K change in scene temperature appears as 0.26 K at the input of the receiver. To measure such small changes in scene temperature, the radiometer must be capable of measuring change that is at least a factor of 5 smaller or $\Delta T = 0.052$ K and that $\Delta T/T_{sys} =$ $0.052/1034.25 = 5.03 \times 10^{-5}$ for the sunlit case and $5.27 \times$ 10^{-5} for the shadowed case. ΔT is called the sensitivity of the radiometer and plays a central role in determining its design and operation.

Another revelation from examinations of these tables is that T_C generates the largest change of 1.5 K in T_{sys} for 1 K change in temperature of the calibration components. To preserve system sensitivity, T_C must be maintained constant to within 0.03 K, or 1 part in 10^4 , for this example.

Impedance match is another significant source characteristic that affects the outcome of radiometer measurement accuracy. There are two aspects to this characteristic: impedance match between hot and cold states, and over the bandwidth of the radiometer. Equations (14), (15) indicate that the *Y*-factor is unaffected if the mismatch over bandwidth is identical for the hot and cold states. Such a condition may be nearly realized by a noise source described below.

Figure 2 shows a filter and amplifier that have the same nominal bandwidth, B. Independent resistive loads are connected to the inputs of both components. The amplifier has gain, G, and noise factor, F. A pair of ganged single-pole-double-throw (SPDT) switches connect either amplifier or filter to an output attenuator, that has loss, L_{Att} . The unconnected component is terminated in a matched load as shown. All the components are housed in a temperature enclosure that is maintained at T_C within the tolerance required for operation as described above. The tight tolerance on temperature ensures the stability of the noise power of the input loads, G, and F of the amplifier, B of both amplifier and filter, loss, L_{Att} , and match of the attenuator, and insertion loss and isolation of the switches. This ensures that the excess noise ratio, ENR, is stable:

$$ENR = \left(\frac{T_C}{T_o}\right) \frac{GF - 1}{L_{Att}} \tag{24}$$

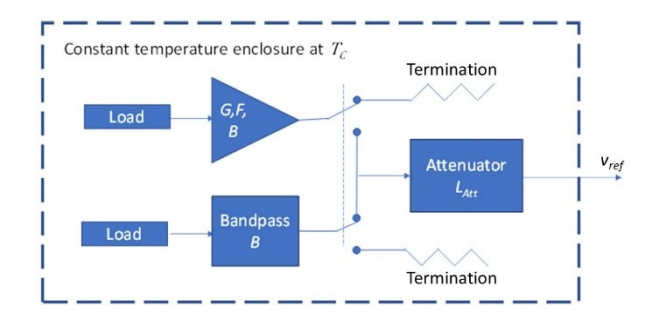


Fig. 2. Conceptual schematic of a noise source that provides nearly identical mismatch in both T_H and T_C states.

A resistive output attenuator provides for both states over the bandwidth B, a constant loss, and, if the loss is high enough (about 20 dB), it provides a nearly constant mismatch that is dominated by the mismatch of the attenuator alone. This is because any mismatch at the amplifier or filter output is attenuated (40 dB in this case) at the attenuator's output. The Bode-Fano criterion [21] imposes a lower bound on the achievable match of the attenuator alone. The best match is achieved by right-sizing the bandwidth to a value that is slightly larger than that of the radiometer. Excessively larger bandwidths lead to poorer achievable attenuator match, and thereby poorer estimates of the gains of the receivers. In some cases, it is expedient to replace the attenuator by a directional coupler with an equivalent coupling value. This approach carries the complications of including the coupler and the antenna feed within the temperature enclosure.

4. CONCLUSIONS

This paper proposes a calibration method of co-located correlation radiometers for the case when cross-coupling between channels can be ignored. We assumed that both channels have the same bandwidth, B, and we described a method to determine the antenna temperature T_A by toggling the reference temperature T_{ref} between hot and cold temperatures. We observe that the toggled temperature of the reference (calibration) source permits calculation of the gains of each channel individually, that is from the measured difference in noise power under hot and cold states. This supplied a basis for equalizing the gains and compensating for the phase difference between channels. We express the antenna temperature T_A in terms of known temperature, T_C , known ENR, and measured Y-factor based on correlation temperature. If the antenna temperature is the same as the reference temperature, the obtained sensitivity of this version of a correlation radiometer is intermediate between the sensitivity of an ideal radiometer and the one for a Dicke radiometer. An analysis is made to illustrate how the operation of the radiometer affects the requirements posed on the source.

5. REFERENCES

- S. Bonafoni, "Microwave Radiometry Imaging for Forest Fire Detection: a Simulation Study," *Progress In Electromagnetics Research*, Vol. 112, 77–92, 2011.
- [2] P. Pampaloni, "Microwave radiometry of forests," Waves in Random Media, 2004, 14.2: S275.
- [3] T. Maeda and T. Takano, "Discrimination of Local and Faint Changes From Satellite-Borne Microwave-Radiometer Data," *IEEE Transactions on Geoscience and Remote Sensing*, 46, 9, pp. 2684-2691, Sept. 2008.
- [4] F. Girard-Ardhuin and R. Ezraty, "Enhanced Arctic Sea Ice Drift Estimation Merging Radiometer and Scatterometer Data," *IEEE Transactions on Geoscience and Remote* Sensing, 50, 7, pp. 2639-2648, July 2012.
- [5] F. Del Frate, P. Ferrazzoli, and G. Schiavon, "Retrieving soil moisture and agricultural variables by microwave radiometry using neural networks," *Remote sensing of environment*, 84.2, 174-183, 2003.
- [6] H. B. Sequeira and C. Nafornita, "Scoping A Document on Recommended Practices For Synthetic Aperture Radiometry," 2023 IEEE International Conference on Acoustics, Speech, and Signal Processing Workshops (ICASSPW), Rhodes Island, Greece, 2023.
- [7] I. Corbella, et al., "The Visibility Function in Interferometric Aperture Synthesis Radiometry," IEEE Trans. on Geoscience and Remote Sensing, Vol. 42, No. 8, 2004, pp. 1667–1682.
- [8] D. E. Weissman, and D.M. Le Vine, "The Role of Mutual Coupling in the Performance of Synthetic Aperture Radiometers," *Radio Science*, Vol. 33, No. 3, 1998, pp. 767– 779.
- [9] C. S. Ruf, C. T. Swift, A. B. Tanner and D. M. Le Vine, "Interferometric synthetic aperture microwave radiometry for the remote sensing of the Earth," in *IEEE Transactions on Geoscience and Remote Sensing*, vol. 26, no. 5, pp. 597-611, Sept. 1988, doi: 10.1109/36.7685.
- [10] S. Weinreb, "New Era Radio Astronomy Science and Technology," presented at the 7th meeting of the IEEE Synthetic Aperture Radiometry Working Group, September 7, 2023.
- [11] Niels Skou, David Le Vine, *Microwave Radiometer Systems:* Design & Analysis, Artech House 2006.
- [12] J.J. Faris, "Sensitivity of a Correlation Radiometer," *Journal of Research of NBS*, vol. 71C, p. 153, June 1967.
- [13] R.H. Dicke, "The Measurement of Thermal Radiation at Microwave Frequencies," Rev. Sci. Instrum., vol.17, pp. 268-275, July 1946.
- [14] B. Laursen and N. Skou, "Synthetic aperture radiometry evaluated by a two-channel demonstration model," *IEEE Transactions on Geoscience and Remote Sensing*, 36, 3, pp. 822-832, May 1998.
- [15] M. Baralis et al., "Calibration techniques and devices for correlation radiometers used in polarization measurements," AIP Conf. Proc. 609, 257–260 (2002).
- [16] I. Pérez et al., "Calibration of Correlation Radiometers Using Pseudo-Random Noise Signals," Sensors, 9, 8, pp. 6131– 6149, Aug. 2009.
- [17] C.Y. Cheng, H. Zhai, "A new calibration standard design for polarization correlation radiometers," 2012 IEEE MTT-S International Microwave Workshop Series on Millimeter Wave Wireless Technology and Applications, 2012.

- [18] H. Brian Sequeira, Corina Nafornita, Peter Vouras, "Calibration of Co-Located Correlation Radiometers for the Case of Crosstalk," 2025 IEEE Conference on Computational Imaging using Synthetic Apertures (CISA), College Park, Maryland, USA, 2-6 June 2025.
- [19] H. B. Sequeira, "An Engineering Introduction to Microwave Radiometry," unpublished.
- [20] G. Evans and C.W. McCleish, RF Radiometer Handbook, Artech House, 1976.
- [21] R. M. Fano, "Theoretical limitations on the broadband matching of arbitrary impedances," Technical Report NO. 41, Research Laboratory of Electronics, MIT, 1948.